

Modeling for Friction of Four Stroke Four Cylinder In-Line Petrol Engine

P.C. Mishra^a

^aSchool of Mechanical Engineering, KIIT University, Bhubaneswar, India.

Keywords:

Friction
Piston subsystem
High performance engine
Firing order
Tribodynamics

ABSTRACT

A four stroke four cylinder in-line petrol engine is modeled to estimate various performance parameters. The solution is based on tribology and dynamics principle. The detailed parameters related to engine friction and lubrication are computed numerically for the 1-3-4-2 engine firing order. The numerical method is based on finite difference method that solves coupled Reynolds Equation and Energy equation. Output includes the film thickness, friction force, friction power loss and temperature rise in ring liner conjunction in all four cylinders. Transient regime of ring liner lubrication is addressed while the same changes from hydrodynamic to mixed in an engine cycle. Momentary cessation near top and bottom dead center that causes boundary interaction is analyzed through asperity contact. The non-Newtonian behavior of lubricant due to film pressure and temperature is addressed using viscosity-pressure-temperature inter relationship.

Corresponding author:

Prakash Chandra Mishra
School of Mechanical Engineering
KIIT University, Bhubaneswar,
India
E-mail: pmishrafme@kiit.ac.in

© 2013 Published by Faculty of Engineering

1. INTRODUCTION

Firing order is the sequence of power delivery of each cylinder in a multi-cylinder IC engine. It is maintained by arranging the ignition (petrol engine) or injection (diesel engine) of fuel in a desired sequence. In modern engines, correct firing order is obtained with an engine management system and/or direct ignition system, which is present in Engine Control Unit (ECU). An appropriate firing order minimizes the vibration, improves the engine balance and allows smooth running of vehicle. Further, it enhances engine fatigue life and passenger comfort. Friction is one important parameter affected by firing order.

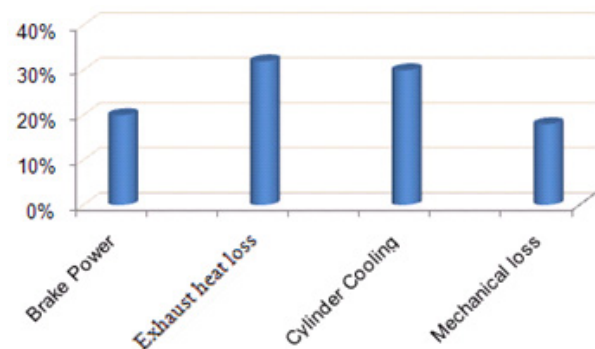


Fig. 1. Energy availability to various engine subsystems (after Taylor [1]).

The energy loss due to friction in an engine as shown in Fig. 1 is the parasitic mechanical loss, which accounts near to 14 % of total input fuel

energy [1]. It happens due to the presence of many relatively moving components; those are in contact while in motion. Such pairs include piston ring-cylinder liner, skirt-liner, piston groove land-ring, small end bearing, big end bearing, and cam-tappet contact. Significant amount of friction loss is due to piston subsystem components in contact [2]. The Fig. 2 represents the piston subsystem components and their possible contact points. In order to avoid the metal-metal contact wear, these relatively moving components are running as lubricated pairs. The mechanism of film formation and its support to minimize contact friction improves engine life. The fluid film has clear effect on film pressure and contact friction [3].

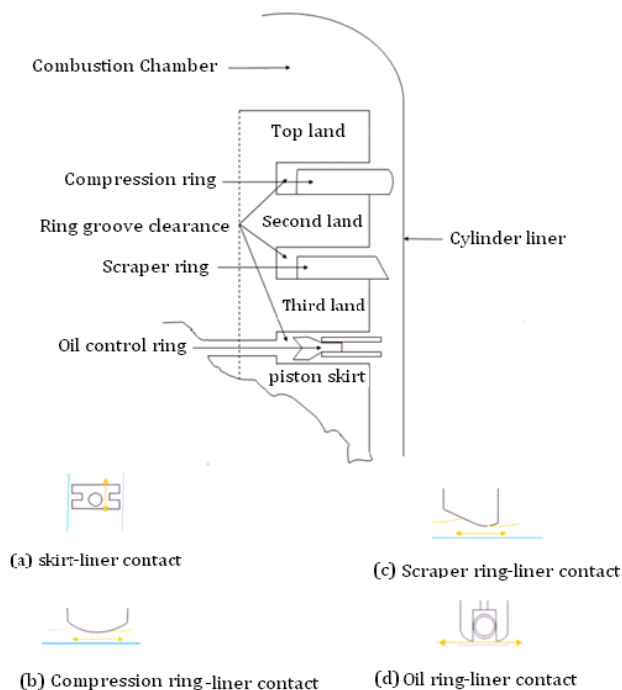


Fig. 2. Piston subsystem components contact profile.

Practically all the relatively moving contiguous surfaces are applied with lubricant to minimize friction and wear. The internal combustion engine (IC engine) components are no exception. Study of Piston subsystem mechanism started with hydrodynamic lubrication of skirt-liner contact [1]. The contact film pressure was predicted by solving a Reynolds equation in such analysis. Subsequently, it is realized that there occurs local or global deformation of ring, liner or skirt due to piston reciprocation. Such phenomena when deformation occurs while lubrication is known as elastohydrodynamics. Ruddy et al [2] carried out elastohydrodynamic lubrication of a twin land type large bored diesel engine oil control ring.

While, dealing with a dynamic piston assembly for lubrication, primary and secondary motion of it largely affect the contact gap. Liu et al. [4] made a comprehensive study of piston assembly and computed the film, friction force, friction power loss due to skirt liner contact. They pointed out the effect of piston skirt profile, engine speed, wrist pin off set and radial clearance on secondary motion of piston considering the parabolic skirt profile.

Earlier it was assumed, the contact friction between piston subsystem components are due to skirt liner contact. Later on, it is realized that not only skirt-liner, but also the rings with liner are main source of friction as reported by Tian et al [5] and Ma et al. [6]. They modeled the performance of piston ring pack. Dynamic behavior of piston ring and its impact on engine friction [7] were studied in these research works.

Piston rings and cylinder liner contact among all contacts of piston subsystem contribute significantly to engine friction loss. Wakuri et al [8] developed a model to study IC engine piston ring friction. The instantaneous friction force of a piston assembly under firing engine conditions was measured by an improved floating liner method. Kim et al [9] studied the effect of lubricating oil film thickness on piston friction of a gasoline engine. Friction is measured using a floating liner in a single cylinder optical engine equipped with sapphire window.

Currently, it is believed that contact conjunction of ring liner is largely influenced by combustion gas pressure [6,12,13]. As the combustion gas pressure shows cyclic variation in an engine with peak value at compression and power stroke transition to almost negligible at suction and exhaust stroke, the lubrication performance parameters varies accordingly.

Piston ring and cylinder contact is subjected to lubrication regime transition. It varies from hydrodynamic to boundary. Also there is mixed regime of lubrication at high pressure zone (300° - 400°) crank angle degree. Pesic et al. [10] developed a method of tribological improvement and testing of piston engine compressor and pump. Through this method, the importance of tribological interface of piston ring and cylinder liner, gas dynamics, piston subsystem contacting

surface coating are highlighted as influences to engine friction loss.

Bolander et al. [11] studied the lubrication regime transition at piston ring and cylinder liner interface. As the friction is more in mixed regime. Akalin and Newaz [12] developed a piston ring and cylinder bore lubrication model for mixed regime of lubrication and compared the numerical results with the experimental results obtained from bench test [13]. They concluded the significant increasing in friction in top and bottom dead center because of high gas pressure and low sliding speed of the piston. The effect of running speed, normal load, contact temperature and surface roughness are investigated.

The numerical method of this model is based on Patir and Cheng [14] method of average flow Reynolds equation. It addresses friction in mixed regime of lubrication. The boundary friction is derived using Tripp and Greenwood [15] model. Spencer et al. [16] developed a semi deterministic roughness model of piston ring and cylinder liner contact.

There are many recent research findings on piston compression ring and cylinder contact. All studies predict more than 80 % of the total friction of piston subsystem is due to compression ring cylinder liner contact. Film thickness, friction force, lubricant temperature change was studied using these models. Santhalia and Kumar [17] studied the effect of compression ring profile on friction force of internal combustion engine.

Temperature change of lubricant due to sliding friction has significant effect on lubrication performance. Mishra [18] and Mishra [19] developed a thermal model for elliptic bore journal bearing. It was based on power law model used by Jang and Chang [20] for a circular journal bearing. Based on such model, Mishra [21] developed a tribodynamic technique addressing transient thermo elastohydrodynamics of piston compression ring and cylinder liner in high pressure zone of engine cycle.

Mishra et al. [22] studied the compression ring tribology at the vicinity of top dead center in compression and power stroke transition.

Further to this Mishra et al [23] developed a numerical model on tribology of piston compression ring in mixed regime and validated the friction with the experimental result of Furuhashi and Sasaki [24].

Based on such broad literature review, it is understood that further research in this area could be the modeling for friction of a four stroke four cylinder engine, which is the finding of this paper.

2. THEORETICAL MODEL FOR FRICTION OF PISTON SUBSYSTEM

At first, the contact geometry of piston rings with cylinder liner is quantified. The film thickness is the sum of minimum gap, contact profile and the deformation (local and or global). Now average flow Reynolds equation is solved for film pressure with help of input parameters such as entraining velocity, lubricant rheology and profile geometry. The film is exact to load and speed condition through load convergence. A FOTRAN90 code is developed to solve the discretized Reynolds equation. It results the film pressure for one crank angle degree. The shear stress is estimated and integrated to obtain friction force. Other parameters like power loss, film thickness etc. are calculated. Further, by varying the crank position and the corresponding combustion pressure and sliding velocity, all these parameters are estimated for the entire engine cycle in all four engines.

2.1 Assumptions of the model

While developing the model, following assumptions are made:

Cylinder bore is textured with cross-h patterned roughness. The piston rings are incomplete circular rings, which are normally larger in dimension compared to the cylinder bore in free state. Installation of the same requires the squeezing of the ring into the cylinder bore, due to which an initial elastic outward force is developed. While in operating state, the combined action of gas pressure force and elastic pressure force is balanced to the lubricant reaction force. While in motion the ring twisting is negligible as the net twisting moment due to all forces is much less than that

due to torsional shear strength of ring material [6].

Non-Newtonian aspect of lubricant is addressed through piezo-viscous equation of viscosity, pressure and temperature interdependency. Synthetic lubricant with high temperature stability is used in these engines.

The entraining velocity is the function of sliding velocity. It is the maximum at mid stroke and zero at dead centers. It has dominant effect in intake and exhaust stroke, but during compression and power stroke, the trend is influenced by higher combustion gas pressure.

Engine components temperature adjacent to the conjunction is assumed to be initial conditions to the further temperature rise. Incremental temperature due to lubricant shear is evaluated by solving the energy equation through power law model.

2.2 Governing equations of the model

The friction in a lubricated contact is the integration of shear stress developed in the lubricant oil due to relative motion of intermediate layers as given in equation (1). Such shear stress has the direct link with the hydrodynamic pressure, oil film thickness and entraining velocity as given in equation (2).

$$F = \iint \tau dx dy \tag{1}$$

Where,

$$\tau = \frac{\eta U}{h} (\phi_{fg} + \phi_{fs}) - \phi_{fp} \frac{h}{2} \frac{\partial p}{\partial x} \tag{2}$$

The hydrodynamic pressure is developed as the film response to separate the approaching contiguous surface. It is estimated by solving the Average flow Reynolds equation as given in equation (3):

$$\frac{\partial}{\partial x} \left(\phi_x \frac{h^3}{12\eta} \frac{\partial p_h}{\partial x} \right) + \frac{\partial}{\partial y} \left(\phi_y \frac{h^3}{12\eta} \frac{\partial p_h}{\partial y} \right) = \frac{U_1 + U_2}{2} \frac{\partial(\phi_g h)}{\partial x} + \frac{U_1 - U_2}{2} \sigma \frac{\partial \phi_s}{\partial x} + \frac{\partial h}{\partial t} \tag{3}$$

As per previous studies, the friction is dominant over the compression and power stroke transition due to higher combustion pressure, which seals the gas. In this mixed regime the hydrodynamic pressure is linked to other parameters through averaged flow Reynolds equation.

Friction force is also affected due to the increase in temperature rise of lubricant. As the viscosity varies due to its interdependency with film hydrodynamic pressure and temperature.

$$\eta = \eta_s e^{\alpha p - \beta \theta} \tag{4}$$

Where,

$$\theta' = \frac{\left[\frac{1}{2} \frac{\partial \theta'}{\partial x^*} - \left\{ \frac{\alpha_{dissipation}}{12} h^{*2} \left(\frac{\partial P^*}{\partial x^*} \right)^2 + \frac{\alpha_{dissipation}}{12} h^{*2} \left(\frac{\partial P^*}{\partial y^*} \right)^2 \right\} \right] - \left[\left\{ \frac{1}{12} h^{*2} \frac{\partial P^*}{\partial x^*} \frac{\partial \theta'}{\partial x^*} \right\} + \frac{\alpha_{dissipation}}{h^{*2}} \right]}{\left[\frac{1}{12} h^{*2} \frac{\partial P^*}{\partial x^*} \frac{\partial \theta'}{\partial x^*} + \frac{1}{12} h^{*2} \frac{\partial P^*}{\partial y^*} \frac{\partial \theta'}{\partial y^*} \right] - \frac{2\alpha_{dissipation}}{h^{*2}}}$$

5)

The momentary cessation of piston assembly occurs near to dead centers. Hence the lubricant film fails to perform due to squeeze only action not enough to maintain separation of contiguous solids. So, boundary interaction is obvious.

$$p_{asp} = K^* E' F_{2.5}(\lambda) \tag{6}$$

where ,

$$K^* = 5.318748 \times 10^{10} \beta_{rk}^{5/2} \tag{7}$$

$$E' = \frac{1}{\left(\frac{1-\nu_1^2}{E_1} + \frac{1-\nu_2^2}{E_2} \right)} \tag{8}$$

And,

$$F_{2.5}(\lambda_{rk}) = \frac{1}{\sqrt{2\pi}} \int_{\lambda_{rk}}^{\infty} (s - \lambda_{rk})^{5/2} e^{-\frac{s^2}{2}} ds \tag{9}$$

The friction mean effective pressure is one important parameter, through which the friction of different engine can be compared. It is given as:

$$P_{mep} = \frac{2P_c(k)}{N.V_d(k)} \tag{10}$$

where,

$P_c(k)$ is the power at k^{th} crank angle, $V_d(k)$ is the displacement volume in cubic meter and N is the engine speed in revolution per second.

2.3 Method of solution and boundary conditions

Method of solution of the model includes following steps:

- Formulation of conjunction geometry and quantification of film shape.
- Derivation of expression for pressure and temperature by centrally differentiating Reynolds equation and energy equation.
- Formation of 180x200 grids for computation purpose by unwrapping the contact surface.
- Initialization of pressure and temperature and computation of further values using an iterative algorithm based on effective influence Newton Raphson method for error convergence.
- Estimation of friction force and friction power loss for all four cylinders.

2.4 Input parameter details

Combustion gas pressure force and the sliding velocity of the piston are two main input parameters. Figures 3 and 4 shows respectively the gas pressure and entraining velocity variation in engine cycle for all the engine cylinders. The gas pressure is measured from a four stroke single cylinder engine with 96 mm bore diameter and 120 mm stroke length, mostly used for high performance application [22].

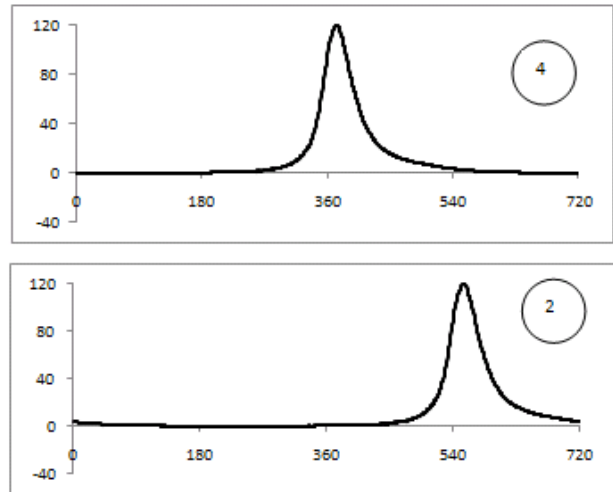
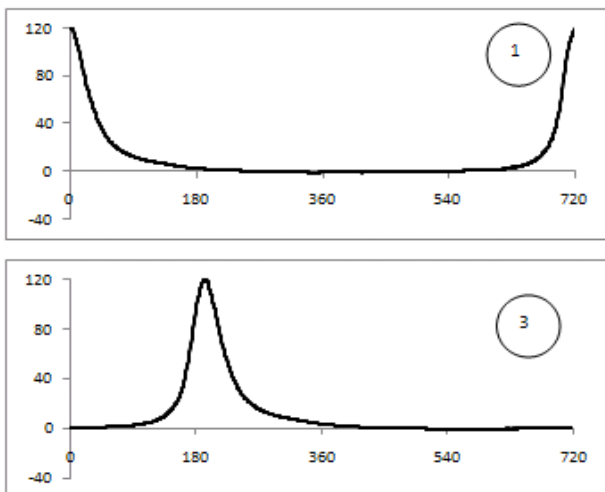


Fig. 3. Variation of combustion gas pressure (in bar) in one engine cycle: in the firing order 1-3-4-2.

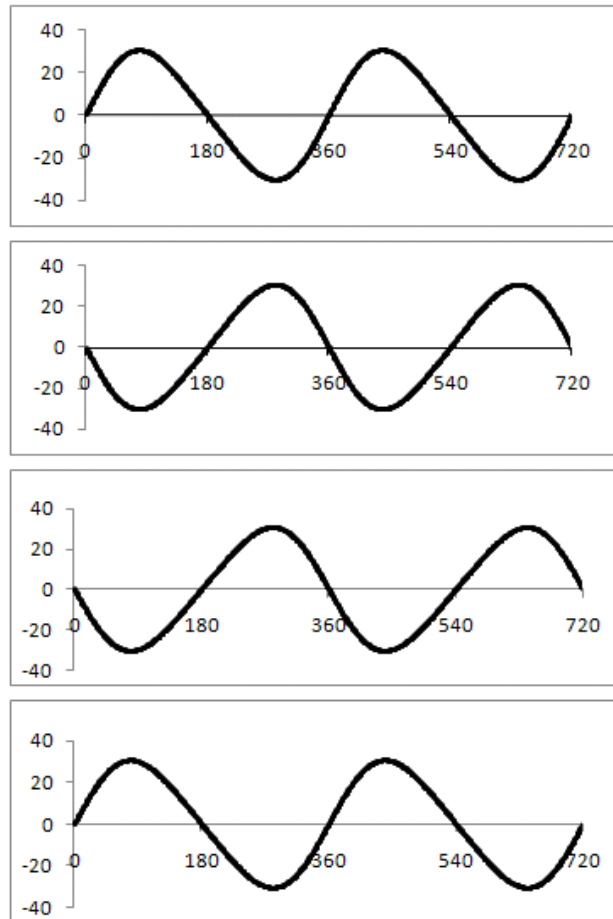


Fig. 4. Cyclic variation of entraining velocity (m/sec): in the firing order 1--3-4-2.

The maximum gas pressure in this case is 120 bars for all four cylinders and the maximum entraining velocity is 36 m/s as the data is used from a high performance engine. All other parameters used in this analysis are enlisted in the Table 1.

Table 1. Details of rings.

Parameters	Value	Parameters	Value
Nominal diameter (mm)	96	Poisson's ratio	0.23
Axial width (mm)	1	Ring moment of inertia (m ⁴)	4.06x10 ⁻¹²
Radial ring depth (mm)	3	Engine operating speed (rpm)	13000
Elastic modulus (GPa)	203	Lubricant dynamic viscosity (PaS)	0.004
Piezo-viscosity index (Pa ⁻¹)	10 ⁻⁸	Number of nodes in axial and circumferential direction	200 and 180

3. VALIDATION OF MODEL

A V8 Chevrolet engine is converted to V2 configuration by Furuhashi and Sasaki [24] with the floating liner in Cylinder 8. The cylinder 7 is left for balancing purpose. The dimensions of the engine are as bore diameter of 94.89 mm, piston stroke of 88.89 mm and pin offset of 1.69 mm. To minimize speed variation, a large flywheel is used. Current model is verified with the experimental result of Furuhashi and Sasaki [24] with speed of 1200 rpm. The friction force validated is presented in Fig. 5.

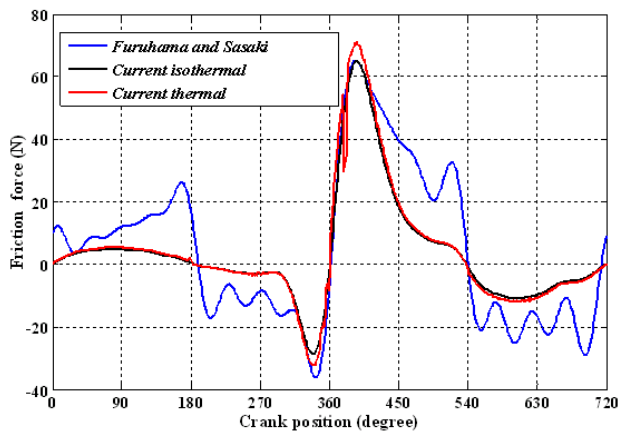


Fig. 5. Model validation for friction force.

Quite good agreement is noted between both the predictions and the measurements. The experimental findings consistently show larger friction than those predicted. Experimental results indicate a greater share for boundary friction, evident by sudden rises at the ends of each stroke.

4. RESULTS AND DISCUSSIONS

The EHL pressure is due to global deformation of the ring. As shown in Fig. 6, the maximum film

pressure developed is around 96 MPa at 120 bar gas pressure. No local deformation occurs due to high ring elastic strength. The Fig. 7 shows the comparison of film thickness in isothermal case to that of thermal case.

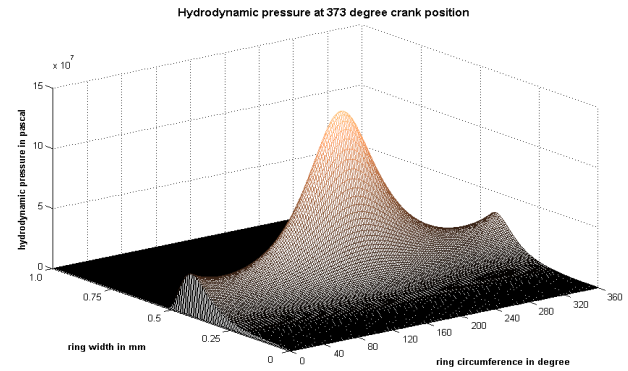


Fig. 6. Elastohydrodynamic film pressure.

For the same operating condition, film computed using thermal condition is less than that computed through isothermal condition.

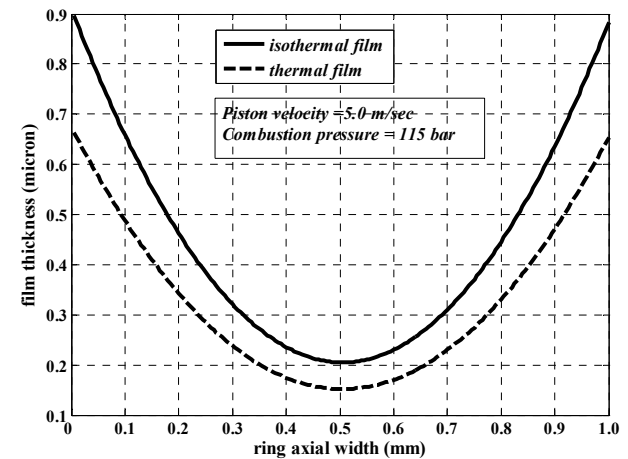


Fig. 7. Film thickness comparison

At any instant of time of the engine operation all four cylinders are under different strokes.

Two cylinders either 1-4 or 2-3 alternatively subjected to high pressure due to compression and power stroke occurred in there (Fig. 3).

Film thickness is near to 6.0 μm during suction and exhaust stroke. Hence regime of lubrication here is hydrodynamic (Fig. 8).

During compression and power stroke the maximum film is about 1.0 μm. While in top dead center (TDC)/bottom dead center (BDC) it falls to 0.3 μm. As such film range is in order of surface roughness, there occurs the boundary friction.

Direction of friction force changes as the direction of piston alters.

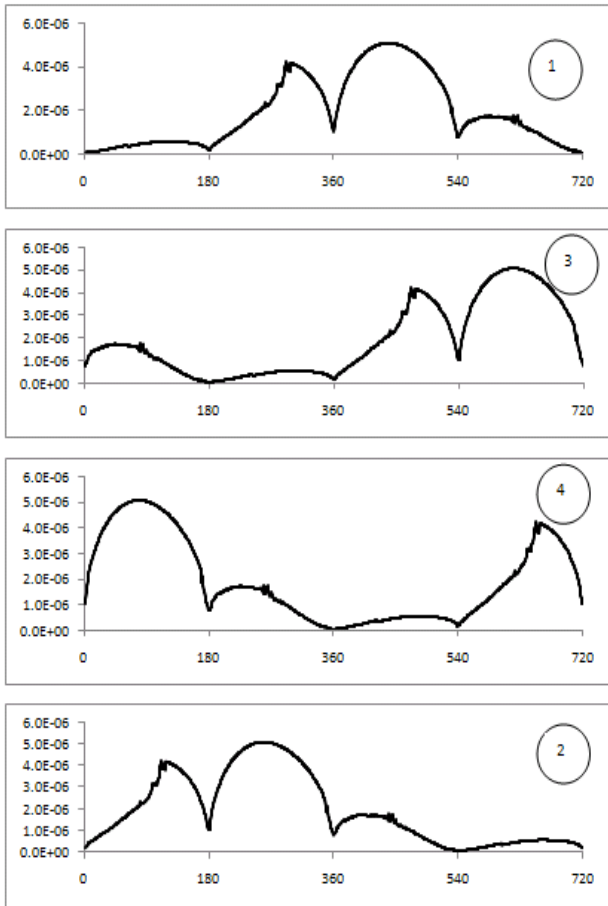


Fig. 8. Film thickness (in micro-meter): firing order 1-3-4-2.

Friction force is higher in compression and power stroke because of mixed or boundary regime of lubrication in contact. Highest value of friction force is 70 N and is in power stroke while that in compression stroke is 20 N.

Friction force is negligible in suction and power stroke. Highest value of friction in these strokes is in order of 5 N.

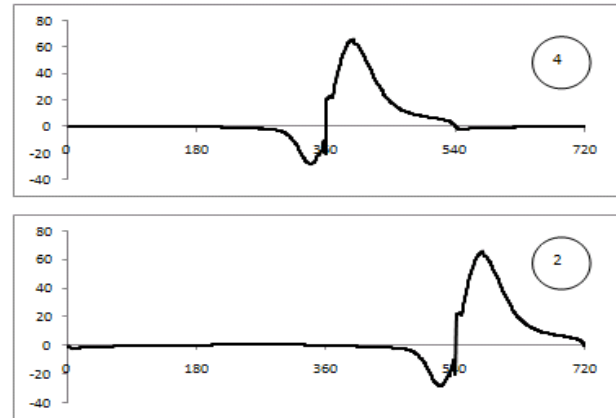
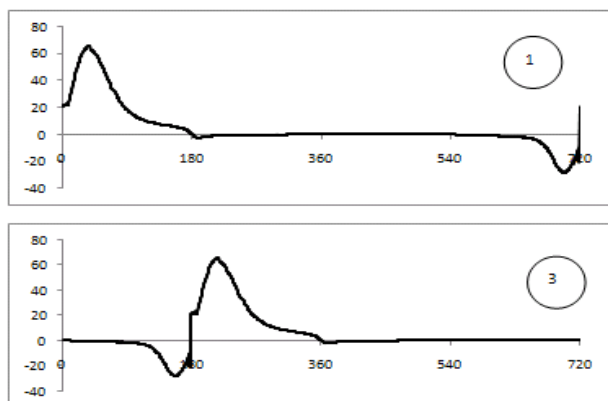


Fig. 9. Engine friction (N) with firing order 1-3-4-2.

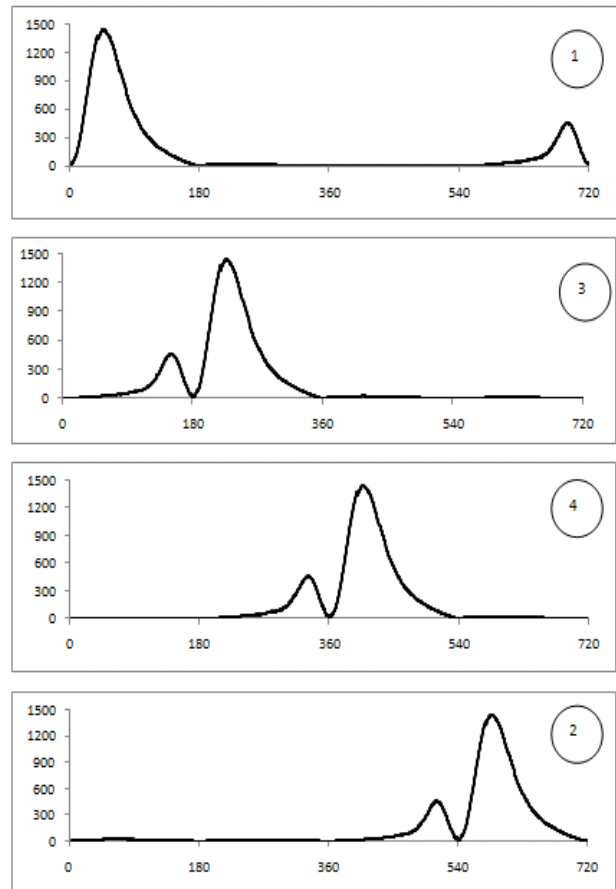


Fig. 10. Frictional power loss (in watt): firing order 1-3-4-2.

Figure 10 shows the cyclic variation of frictional power of four cylinder engine with fire order 1-3-4-2. The maximum frictional power loss being 1500 watt in power stroke. It is 400 watt in compression stroke.

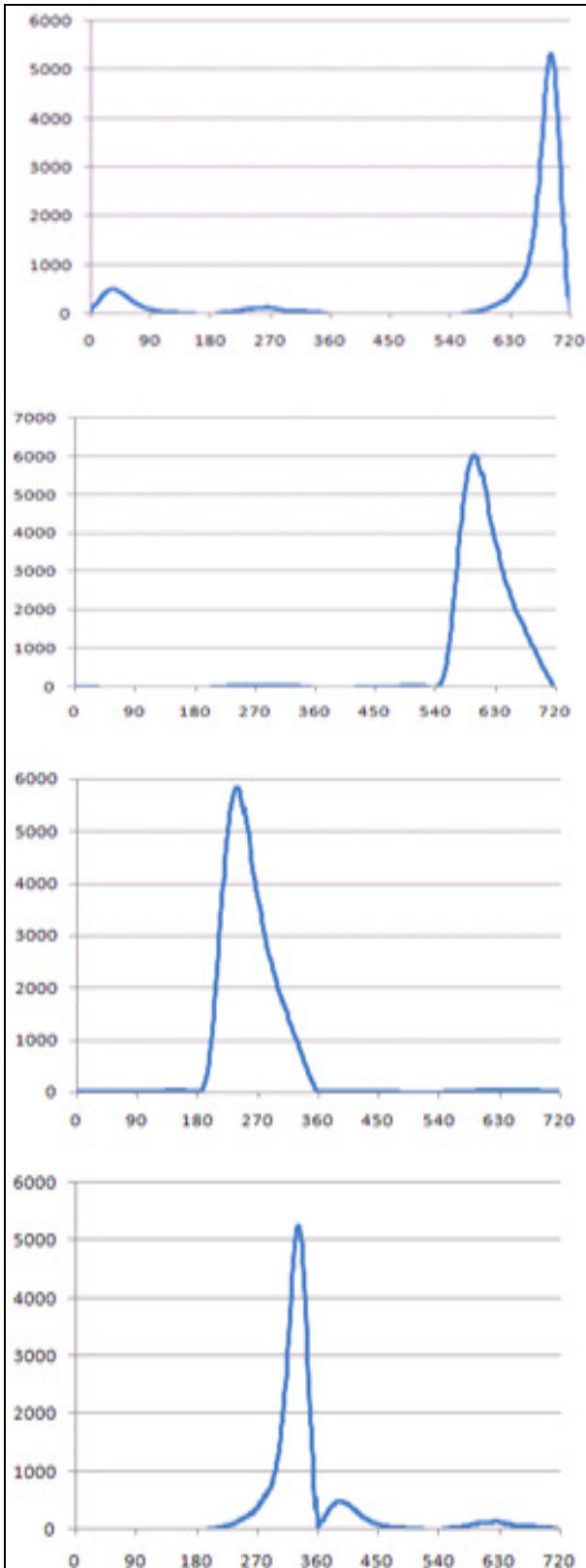


Fig. 11. Friction mean effective pressure (in N/m²) with firing order 1-3-4-2.

Figure 11 shows the variation of friction mean effective pressure in an engine cycle for firing order of 1-3-4-2. Highest being 6000 N/m² during power stroke.

5. CONCLUSION

A four stroke four cylinder engine is modelled for lubrication performance. The friction force obtained is validated with the experimental results obtained from Furuhashi and Sasaki [24]. Lubricant film between ring and liner is sufficient enough (1 to 6 μm) to maintain gap in suction and exhaust stroke. Compression and power stroke especially 300^o-400^o crank location due to higher order of combustion gas pressure. The contact experiences mixed regime where the liner and ring roughness plays an important role. To avoid friction and subsequent wear, the liner surface is textured with cross h pattern and the ring is coated with thermal and wear resistant coatings.

The future investigation of this work leads to thermal effect in engine lubrication, wear monitoring of high performance engines. Such studies will significantly improve the current state of art engine tribology.

Nomenclature

E	Modulus of elasticity of the ring	Nm^{-2}
E'	Reduced modulus of elasticity of the contacting pair	Nm^{-2}
$F_{2.5}(\lambda_{rk})$	Gaussian function of asperity distribution	
F	Friction Force	N
h_0, h	Gap, Film thickness	μm
K^*	Constant used in calculation of asperity contact pressure	
p_{asp}	Asperity contact pressure	
$P_c(k)$	Frictional power loss in crank location k	watt
p_{mep}	Friction mean effective pressure	N/m^2
$s_{i,j}$	Undeformed axial ring profile	m
t	Time	sec
U	Speed of entraining motion	ms^{-1}
V	Speed of side-leakage	ms^{-1}
W	Contact load (integrated pressure distribution)	N
x, y	Co-ordinate directions	
θ^*	Non-dimensional temperature	
$\alpha_{dissipation}$	Coefficient for heat dissipation	
β_{rk}	Parameter used in calculation of asperity contact pressure	
η	Lubricant dynamic viscosity	Pas
\mathcal{G}	Damping factor	

σ	Parameter used for calculating flow factor	
γ_c	Surface pattern parameter	
λ_{rk}	Stribeck's oil film parameter	-
$\left(\begin{matrix} \phi_p, \phi_s, \\ \phi_g, \phi_{fg}, \\ \phi_{fp}, \phi_{fs} \end{matrix} \right)$	Flow factors of geometry, pressure and shear	
ρ	Lubricant density	kgm^{-3}
τ	Shear stress	Nm^{-2}

REFERENCES

[1] C.M. Taylor: *Fluid Film Lubrication in the Internal Combustion Engine*, Journal of Physics D: Applied Physics, Vol. 25, No. 1A, pp. A91, 1992.

[2] G.D. Knoll, H.J. Peeken: *Hydrodynamic Lubrication of Piston Skirt*, Journal of Lub. Technol., Vol. 104, No. 4, pp. 505-509, 1982.

[3] B. Ruddy, D. Dowson, P.N. Economou: *The Prediction of Gas Pressure within Ring Packs of the Larger Bore Diesel Engine*, Journal of Mech. Eng. Sci., Vol. 23, No. 6, pp. 295-304, 1981.

[4] K. Liu, Y.B. Xie, C.L. Gui: *A Comprehensive Study of the Friction and Dynamic Motion of Piston Assembly*, Proc. IMechE, Part. J: J. Engng. Tribol., Vol. 212, pp. 221-226, 1998.

[5] N. Patir, H.S. Cheng: *Application of Average Flow Model to Lubrication between Rough Sliding surfaces*, Trans ASME J Lub Technol, Vol. 101, pp. 221-230, 1979.

[6] M.T. Ma, S. Smith, I. Sherrington: *A three dimensional analysis of piston ring lubrication, Part 1: Modelling*, Proc. IMechE, Part. J: J. Engng. Tribol., Vol. 209, pp. 1-14, 1995.

[7] T. Tian: *Dynamic Behavior of Piston Rings and their Practical Impact, Part-I: Ring Flutter and Ring Collapse and their Effects on Gas Flow and Oil Transport*, Proc. Instn. Mech. Engrs. Part J: J. Engg. Tribol, Vol. 216, pp. 209-228, 2002.

[8] Y. Wakuri, T. Hamatake, M. Soejima, T. Kitahara: *Piston ring friction in internal combustion engines*, Tribology International, Vol. 25, No. 5, pp. 299-308, 1992.

[9] K.S. Kim, T. Godward, M. Takiguchi, S. Aoki: *Part 2: The effects of lubricating oil film thickness distribution on gasoline engine piston friction*, SAE 2007-01-1247, 2007.

[10] R. Pesic, A. Davinic, S. Veinovic: *Methods of tribological improves and testing of piston engines, compressors and pumps*, Tribology In Industry, Vol. 27, No. 1&2, pp. 38-47, 2005.

[11] N.W. Bolander, B.D. Steenwyk, F. Sadeghi, G.R. Gerber: *Lubrication Regime Transitions at the Piston Ring-Cylinder Liner Interface*, Proc. IMechE., Part.J: J. Tribol., Vol. 219, No. 1, pp.19-31, 2005.

[12] O. Akalin, G.M. Newaz: *Piston Ring Cylinder Bore Friction Modelling in Mixed Lubrication Regime: Part. I-Analytical Results*, ASME J. Tribol., Vol. 123, No. 1, pp. 211-218, 1999.

[13] O. Akalin, G.M. Newaz: *Piston Ring Cylinder Bore Friction Modelling in Mixed Lubrication Regime: Part. II-Correlation between Bench Test Data*, ASME J. Tribol., Vol. 123, pp.219-223, 2001.

[14] N. Patir, H.S. Cheng: *Application of Average Flow Model to Lubrication between Rough Sliding surfaces*, Trans ASME J Lub Technol, Vol. 101, No. 2, pp. 220-229, 1979.

[15] J.A. Greenwood, J.H. Tripp: *The Contact of Two Nominally Flat Surfaces*, Proc. Inst. Mech. Engng., Vol. 185, No. 1, pp. 625-633, 1970.

[16] A. Spencer, A. Almqvist, R. Larsson: *A semi deterministic texture-roughness model of the piston ring-cylinder liner contact*, Proc Instn Mech Engrs Part J: J Engg Tribol, Vol. 225, No. 6, pp. 325-333, 2011.

[17] A. Sonthalia, C.R. Kumar: *The Effect of Compression Ring Profile on the Friction Force in an Internal Combustion Engine*, Tribology in Industry, Vol. 35, No. 1, pp. 74-83, 2013.

[18] P.C. Mishra: *Thermal analysis of elliptic bore journal bearing considering shaft Misalignment*, Tribology Online, Vol. 6, No. 5, pp. 239-246, 2011.

[19] P.C. Mishra: *Mathematical modeling of stability in rough elliptic bore misaligned journal bearing considering thermal and Non-Newtonian effect*, Applied Mathematical modeling, Vol. 37, No. 8, pp. 5896-5912, 2013.

[20] J.Y. Jang, C.C. Chang: *Adiabatic analysis of finite width journal bearing with non-Newtonian lubricant*, Wear, Vol. 122, No. 1, pp. 63-75, 1988.

[21] P.C. Mishra: *Tribodynamic modeling of piston compression ring cylinder liner contact at high pressure zone of engine cycle*, The International Journal of Advances in Manufacturing Technology, Vol. 66, No. 5-8, pp. 1075-1085, 2013.

[22] P.C. Mishra, H. Rahnejat, S. Balakrishnan: *Tribology of compression ring-to- cylinder contact at reversal*, Proc Instn Mech. Engrs., Part J: J.Engng Trib., Vol. 222, No. 7, pp. 815-826, 2008.

[23] P.C. Mishra, H. Rahnejat, P.D. King: *Tribology of the ring-bore conjunction subject to a mixed regime of lubrication*, Proc Instn Mech. Engrs., Part C: J. Mech. Engng Sci, Vol. 223, No. 4, pp. 987-998, 2009.

[24] S. Furuhashi, S. Sasaki: *New Device for the measurement of Piston Frictional Forces in small engines*, Society of Automotive Engineers, SAE 831284, pp. 39-50, 1983.